PHYSICS AND CHEMISTRY OF SOLID STATE
V. 27, No. 1 (2026) pp. 52-61
Section: Physics

DOI: 10.15330/pcss.27.1.52-61

Vasyl Stefanyk Carpathian National University

ФІЗИКА І ХІМІЯ ТВЕРДОГО ТІЛА
Т. 27, № 1 (2026) С. 52-61
Фізико-математичні науки

PACS: 28.52.Fa; 61.05.-a; 66.70.-f ; 81.05.Je; 89.75.Kd

ISSN 1729-4428 (Print)
ISSN 2309-8589 (Online)

A.S. Shirinyan[1], L.V. Marynchenko[2], O.I. Nizhelska[1]

A Fractal Approach to Evaluating the Thermal Conductivity of ZrB_2–C Composite Ceramic Materials

[1]*Laboratory of composite materials for nuclear-hydrogen energy, Institute of Applied Physics of National Academy of Sciences of Ukraine, Sumy, Ukraine, aramshirinyan@ukr.net*
[2]*Department of Bioenergetic, Bioinformatic and Ecobiotechnology, National Technical University of Ukraine "Igor Sikorsky Kyiv Polytechnic Institute", Kyiv, Ukraine, lolitamar@ukr.net*

A pressing issue in materials science is the controlled application of ceramic composite materials at high temperatures in modern technologies, particularly in nuclear physics, atomic energy, aerospace, and rocket engineering. This study investigates the correlation between the thermal conductivity of synthesized ZrB_2–C ceramic composites and their microstructural features using fractal analysis. The composites were produced via high-temperature reactive synthesis from boron and zirconium carbide powders. Scanning electron microscopy (SEM) and backscattered electron (BSE) modes was used to obtain micrographs of the fracture surfaces. These images were analyzed using the *Box Counting* method with *ImageJ* and *FracLac* software to determine two fractal parameters: fractal dimension and lacunarity. A strong inverse correlation was observed between lacunarity and thermal conductivity. The study demonstrates that fractal analysis, particularly the lacunarity parameter, can serve as a useful tool for assessing heat transfer potential in two-phase ceramic composites, especially when conventional measurement methods are impractical.

Keywords: ceramic composites, boron carbide, zirconium carbide, zirconium diboride, graphite, microstructure, fractal analysis, thermal conductivity, lacunarity, energy industry.

Received 28 October 2025; Accepted 14 January 2026; Published 07 February 2026.

Introduction

Establishing the relationship between the structure of a material and its physical properties is a key challenge in materials science. A material with the same chemical composition, but differing in grain size, pronounced anisotropy, porosity, and other structural features, can exhibit significantly different optical and mechanical properties [1].

For composite materials consisting of two or more phases that undergo transformations during chemical reactions, the number of possible structural configurations increases significantly. In addition, such materials may be subjected to mechanical, thermal, and radiation-induced stresses. In this case, establishing a correlation between the microstructure and the macroscopic properties of the material becomes even more complex, requiring the application of alternative research methods. For example, in nuclear power engineering, this includes techniques for monitoring the parameters of reactor cladding materials [2]. This is particularly relevant for the measurement and characterization of the thermal conductivity of composite materials used in nuclear applications.

Experimental objects often exhibit irregular local structures and certain self-similar (automodel) properties. In specific cases, it is possible to describe the structure of a material in a mathematically averaged manner using fractal analysis of microscopic images [3]. A key characteristic of fractals that enables a quantitative assessment of their complexity is the fractal dimension, *D*. This parameter reflects the irregularity and non-standard shape contours of the structure. For two-dimensional images, *D* typically ranges between 1 and 2, with more complex patterns corresponding to higher values of *D*. This makes fractal dimension a valuable tool in various

scientific and applied studies [4–5], particularly for texture defect monitoring [3].

Within the framework of fractal analysis, lacunarity *L* has also been identified as an important structural parameter. It characterizes how densely a fractal fills space and reflects the degree of structural heterogeneity [6–7].

For a common type of disordered two-phase composites several attempts have been made to predict the thermal conductivity of such materials as a function of filler content. In particular, approaches have been proposed that explain the thermal conductivity of composites in terms of the fractal geometry of the conductive phase embedded within the matrix material [8]. However, the influence of the geometric microstructure of the thermally conductive phase – which governs heat transfer in two-phase composites – remains a complex and insufficiently studied issue for disordered systems. Therefore, there is a pressing need to develop an effective method for determining thermal conductivity as a function not only of the filler content, but also of the geometrical microstructure of the dispersed phase. In this context, a quantitative assessment of the geometric characteristics of the second phase plays a crucial role in explaining the thermal conductivity behaviour of the composite.

The characterization of composite materials under various manufacturing or operational conditions requires standardized imaging of samples, calculation of their fractal parameters, and correlation of these parameters with technologically important physical properties.

In [9], a quantitative fractal analysis was performed on the grain boundaries of the microstructure of steel used in oxygen cylinders with service lifetimes ranging from 18 to 55 years. The obtained values of the fractal dimension ranged from 1.10 to 1.14. High non-linear correlations (with a maximum) were observed between the fractal dimension and impact toughness, destructive pressure during hydrotesting, and the conditional yield strength.

In [2], the task of real-time automated monitoring of the hermeticity of fuel element cladding in nuclear reactor assemblies was addressed. The authors proposed a method for assessing the surface quality of the cladding material and detecting failure of the fuel element based on the fractal dimension of damage and fracture defects on the surface of the cladding.

As a result of high-temperature chemical reactions between the initial components of a composite, a new phase may form. For example, in cast irons used for producing castings, the interaction of silicon with carbon monoxide during solidification leads to the formation of silicon monoxide and graphite crystals. Graphite formation typically occurs at the phase boundary. A review of the literature allows for the following conclusions:

Graphite inclusions in materials synthesized through high-temperature reactions exhibit a wide variety of morphologies – from regular spherical shapes to branched dendrites composed of thin flakes. The morphology of graphite depends significantly on the conditions of synthesis and processing, such as chemical composition, pressure, cooling rate, and even the shape of the mold used for the sample [10–11];

The shape of graphite inclusions can be used to predict the macroscopic properties of the material, such as impact resistance, vibration damping capacity, and thermal conductivity [12];

This conclusion is also supported by three-dimensional numerical models that establish the relationship between microstructure and the thermomechanical behavior of materials [13–14].

Fractal models of thermal conductivity primarily focus on porous media [13–14]. However, it can be assumed that a similar approach could be applicable to multiphase composite ceramics in which the constituent phases exhibit significant differences in thermal conductivity. From this perspective, fractal analysis of the resulting material structures may serve as a useful tool for evaluating key material properties — such as thermal conductivity — especially when the thermal conductivities of the individual phases differ substantially.

One of the most promising materials in nuclear physics, nuclear energy, and aerospace and rocket engineering is zirconium diboride (ZrB_2) due to its high melting point, oxidation and thermal shock resistance, thermal conductivity, and relatively low density (which helps reduce the weight of structural components) [15–16]. Experimental data indicate that the thermal conductivity of ZrB_2 at room temperature ranges from 56W/(m·K) to 133W/(m·K), depending on the presence of microimpurities [17]. For zirconium carbide (ZrC), the thermal conductivity ranges from 11.6W/(m·K) to 25W/(m·K), influenced by factors such as material density, the concentration of carbon vacancies, and impurities [18]. For graphite, thermal conductivity lies approximately in the range of 119–165 W/(m·K) and can vary significantly depending on the crystallographic direction [19]. In the case of boron carbide (B_4C), values typically fall between 100W/(m·K) and 125W/(m·K) [20]. These data demonstrate a strong dependence of thermal conductivity on impurity concentration, with values potentially varying by a factor of two. Therefore, the search for correlations between the structural-phase composition and operational thermophysical properties is a highly relevant task for such composite materials [21]. To the best of our knowledge, a fractal analysis of a ZrB_2–graphite-based composite has not yet been conducted.

The aim of this work is to investigate the influence of the microstructure of the ZrB_2–C ceramic composite, obtained by high-temperature reactive synthesis from boron and zirconium carbide powders, on the thermal conductivity coefficient using fractal analysis methods.

I. Materials and methods

1.1. Sample preparation methodology using powder metallurgy techniques

Composite material samples were produced from a mixture of boron and zirconium carbide powders by the method of reactive hot pressing, as described in [22]. As starting materials, powders from two institutions were used: ZrC (99% purity with an average grain size of 5 μm) and B_4C (98.5% purity with an average grain size of 20 μm) – from the Donetsk Reactive Factory (Ukraine); and B_4C (99.5% purity with a mean grain size of 2 μm) –

from Sigma Aldrich (USA). Thus, the initial composition differed only in the type of B_4C – two types of boron carbide were used, with different levels of purity and different powder grain sizes.

The ratio of compounds in the starting powders was calculated based on the main solid-state chemical reaction in such a way that, in the resulting samples, the components would fully react (x=2)

$$xZrC_{0.8} + B_4C \rightarrow 2ZrB_2 + (x-2)ZrC + 2.6C,$$

$$2ZrC_{0.8} + B_4C = ZrB_2 + 2.6C.$$

As a result, four types of composite ceramics were obtained. The fabrication conditions for the composite materials from the initial mixture differed only slightly: under the general conditions of reactive synthesis, the powders were sintered at a temperature of 1900°C for 4–8 minutes under a pressing pressure of 30 MPa. A detailed description and the exact fabrication technology of the composite materials are not disclosed due to patent-related considerations.

The thermal conductivity coefficient (hereafter referred to as *k*) was measured using the method described in [23], at room temperature, with the following results: sample № 1 – $k = 43.3 \pm 1$ W/(m·K), sample № 2 – $k = 71.7 \pm 5$ W/(m·K), sample № 3 – $k = 41 \pm 1$ W/(m·K), sample № 4 – $k = 67.5 \pm 5$ W/(m·K). Microimages of the samples and the thermal conductivity data were provided by Dr. Oleksii Popov (Institute of Applied Physics, Sumy, Ukraine; Institute of Materials Research, University of Huddersfield, UK).

Sample fragments were obtained from the ZrB_2–C ceramic composites by a hummer impact, and the fracture surfaces of these samples were examined using scanning electron microscopy (SEM). Microimages of the surface structure were acquired using a Tescan Vega3 microscope (Czech Republic) in two modes:

1) secondary Electron (SE) mode (SEM – Scanning Electron Microscope), which provides high-resolution images of the sample surface and is sensitive to surface topography;

2) backscattered Electron (BSE) mode (BSEM – Backscattered Electron-Scanning Electron Microscope), which provides information about the atomic composition of the surface, as the elastic backscattering of electrons depends on the atomic mass of the material.

1.2. Image Processing Methodology

The obtained microimages were analyzed at various magnifications using the *ImageJ* software and the *FracLac* plugin, applying the *Box Counting* method with default settings. This method involves counting the number of squares *N* of side length *r* required to cover the contours of shapes in the image after it has been converted to black and white (binarization); *N* is expressed as a function of *r*. The slope of the logarithmic dependence between *N* and *r* represents the fractal dimension *D* of the image. The greater the value of *D* (ranging from 1 to 2 for a 2D plane), the more complex the image pattern and the more it deviates from a simple geometric figure.

Although this method yields fractal dimension values that may deviate from those of ideal figures (such as a line or a circle), for which the exact mathematical values are known, it is nonetheless suitable for evaluating real complex physical objects [24, 25].

Identical values of the fractal dimension do not necessarily indicate similarity in image patterns. Therefore, an additional parameter for evaluating the microphotographs, also determined using the *FracLac* plugin, was lacunarity (*L*). This metric allows for assessing the heterogeneity of void (lacuna) distribution in the material's texture. A low lacunarity value indicates a more uniform distribution of voids, while a high value suggests the presence of larger voids and/or uneven localization.

The *L* parameter for real objects is scale-dependent, since at lower magnification the surface appears more homogeneous. In such cases, the *L* value may vary significantly more than the fractal dimension *D* [24–25]. Thus, fractal analysis was performed by comparing the images of the samples at the same magnification scale.

The statistical error for the fractal dimension *D* was determined automatically by the software as the standard deviation, while the error for lacunarity *L* was calculated separately within a 95% confidence interval based on the number of values obtained. The multiple correlation coefficient R^2 was approximately 0.99 for both parameters.

In total, images of four composite material samples were analyzed. These differed in manufacturing conditions and in the imaging modes used – SE and BSE. The thermal conductivity coefficient *k* of the ZrB_2–C composite material was compared with the calculated fractal parameters *D* and *L*, which reflect the microstructure of the respective sample.

II. Results

2.1. Visual Description of Sample Images

The microimages of the composite samples differed visually from one another (Figs. 1–2 and 4 at 10 μm scale, and Fig. 3 at 5 μm scale). In the SE images, the main grains of the ZrB_2 matrix appear in gray and light-gray shades, graphite is visible as dark areas between the matrix grains or as small dark rounded inclusions on the matrix grains. In the BSE images, the main ZrB_2 matrix appears in a light-gray shade, while the dark phase indicates the presence of graphite. Compared to SE images, BSE images exhibit significantly less grayscale gradient, i.e., they appear more uniformly shaded.

In the SE images, bright (light) rims are sometimes visible at the boundaries of some matrix grains, corresponding to zones where thin graphite flakes have segregated. These inclusions are not visible in the BSE images due to the small thickness of the graphite flakes and the characteristics of the imaging mode.

Let us consider the image of Sample №1 (magnification 10k× in Fig. 1). In the SE images, the ZrB_2 matrix grains can be seen to vary in size (from 1.5 to 9 μm) and shape. Some grains appear as conglomerates (large agglomerations). The SE images also show slightly brighter (white) rims of graphite at the boundaries of these conglomerates, possibly indicating the segregation of thin graphite flakes [11]. The thickness of these bright rims is

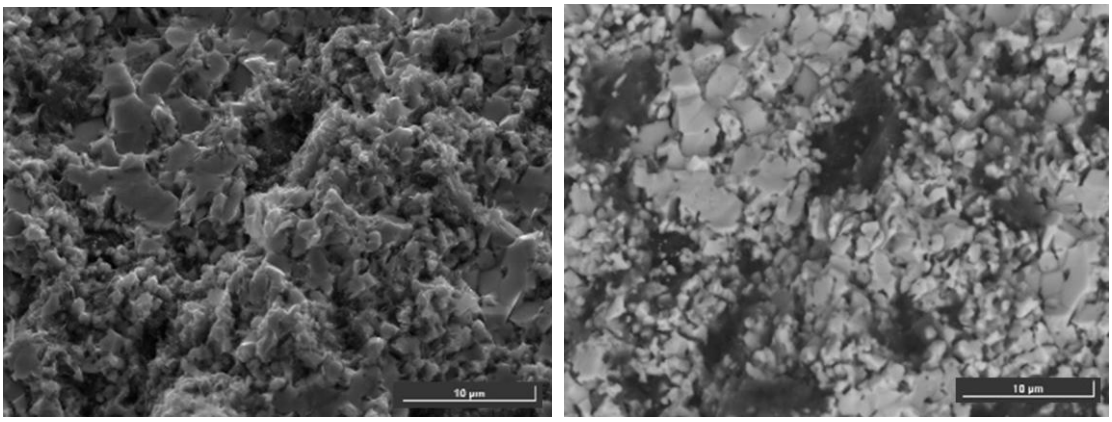

(a) (b)

Fig. 1. Microimage of the fracture surface of Sample №1 at 10k× magnification: (a) in SE mode, (b) in BSE mode.

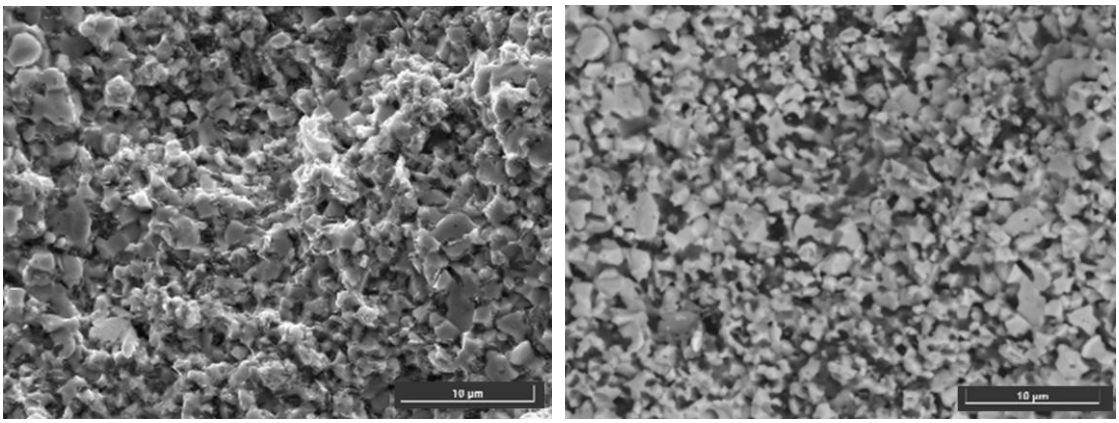

(a) (b)

Fig. 2. Microimage of the fracture surface of Sample №2 at 10k× magnification: (a) in SE mode, (b) in BSE mode.

estimated to be a few nanometers. Due to elastic scattering, such thin graphite rims are not detectable in the BSE images. In the SE images, within the gaps between the ZrB_2 matrix grains, compact dark zones ("islands") of graphite are observed, ranging in size from 1 to 10 µm and irregular (elongated) in shape, distributed unevenly. In the BSE images, the main zirconium diboride matrix appears light gray, while the dark zones indicate graphite.

Let us consider the image of Sample № 2 (magnification 10k×, Fig. 2). In this case, the SE images show that the grains of the main ZrB_2 matrix are smaller (in comparison with Sample №1). In addition, a visual comparison with Sample №1 suggests that the size distribution of the ZrB_2 grains is narrower, with grain sizes ranging from 1.5 to 4 µm. The grain shapes are predominantly irregular. The dark graphite particles are also smaller, with estimated sizes between 1 and 2.5 µm; they are irregular in shape and distributed in a relatively uniform yet chaotic manner. In the SE image, the boundaries of many matrix grains are surrounded by white rims, which may indicate active zones of graphite flake formation [11]. In the BSE image, the ZrB_2 matrix grains appear light gray, while the carbon phase appears dark gray to black.

Let us consider the image of Sample № 3 (magnification 20k× in Fig. 3). Again, in the SE image the ZrB_2 matrix grains are smaller than those in Sample № 1 (estimated to be between 1.5 and 5 µm), with irregular and sometimes elongated shapes. Bright rims of graphite flakes are again observed on some grains. The main graphite inclusions are also smaller than in Sample № 1, but larger than in Sample № 2 (estimated between 2 and 6 µm), and are arranged in compact "islands".

In the SE microimage of Sample №3 (Fig. 3a), small white grains can be seen (estimated between 0.2 and 1.5 µm) with irregular, peculiar shapes (highlighted in the inset). It can be assumed that these particles are either unreacted ZrC powder or other impurities, possibly originating from the starting powder used for Sample № 3. In the BSE image, these grains do not differ in contrast from the main matrix, indicating similar atomic number characteristics. Thus, Sample №3 can be considered an example of an incomplete reaction, where the number of phases in the composite exceeds two.

Let us consider the image of Sample № 4 (magnification 10k× in Fig. 4). The matrix grains are more rounded and smaller than those in Sample № 1, approximately 2–4 µm in size, with lower size dispersion. Also, compared to Sample № 1, the graphite inclusions in the SE image are even smaller (estimated at 0.5–1.5 µm) and are distributed uniformly. The BSE image also shows a noticeable reduction in the size of both the matrix grains and the graphite phase (in comparison with Sample № 1).

2.2. Fractal Parameters of the Images of the Obtained Composites

The obtained SE and BSE microimages were analyzed using the Box Counting method, and the fractal

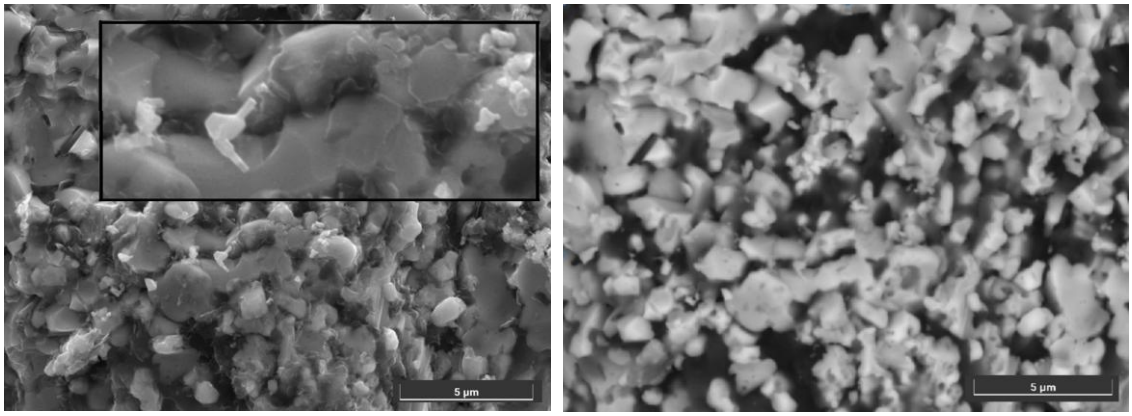

(a) (b)

Fig. 3. Microimage of the fracture surface of Sample №3 at 20k× magnification:(a) in SE mode, (b) in BSE mode.

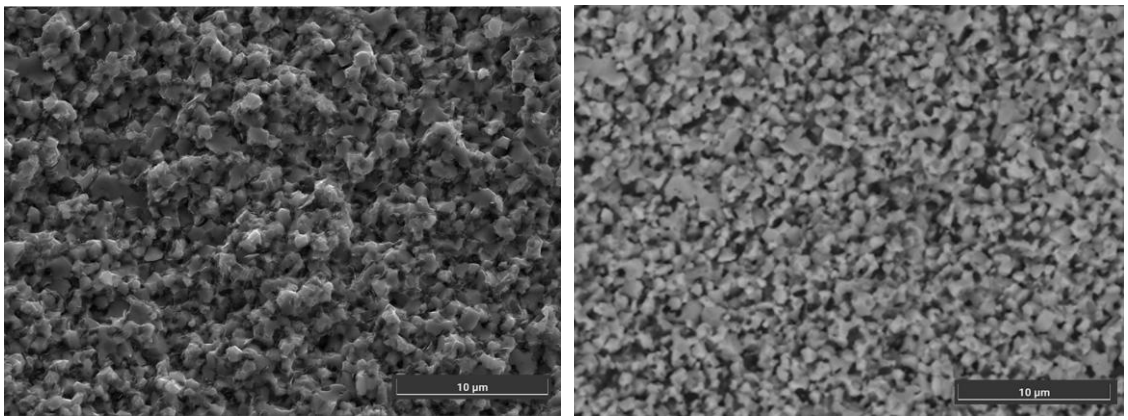

(a) (b)

Fig. 4. Microimage of the fracture surface of Sample №4 at 10k× magnification:(a) in SE mode, (b) in BSE mode.

dimension D and lacunarity L were determined (Table 1).

III. Discussion

Let us compare the fractal dimension of the microimages for different samples at the same magnification. For example, we select the case of 10k× magnification and SE images (Table 1). The data show that: $D = 1.790 \pm 0.035$ for Sample № 1, $D = 1.804 \pm 0.034$ for Sample № 2, $D = 1.812 \pm 0.035$ for Sample № 3, $D = 1.821 \pm 0.037$ for Sample № 4. Thus, it can be observed that the value of the fractal dimension D increases: it is the lowest for Sample №1 and the highest for Sample № 4. This trend is consistent across all fixed magnifications, indicating a slight (within the margin of error) increase in texture complexity from Sample № 1 to Sample № 4. This may be related to the reduction in grain sizes of both zirconium diboride and graphite in the corresponding samples.

At the same time, the variation in D across all samples is relatively small compared to the error margin of the *Box Counting* method. This limitation reduces the usefulness of the fractal dimension D as a quantitative evaluation factor and highlights the need for an additional parameter L. The data show that the changes in lacunarity values exceed the measurement error.

The relevance of choosing lacunarity L is also supported by the need to account for the distribution of the primary matrix and graphite phases: lacunarity allows to distinguish between the two end phases ─ ZrB_2 and C (as two colors) ─ in a two-phase system, whose distribution directly affects the material's thermal conductivity.

In Fig. 5, we present the correlation between fractal dimension and lacunarity based on the data from Table 1. As can be seen, there are linear relationships with high coefficients of determination. Therefore, in the following analysis, we will use lacunarity as a quantitative metric for evaluation and for establishing correlations with thermal conductivity.

Let us examine the issue of selecting image magnification for comparison and evaluation. The calculated fractal parameters from SE and BSE microimages show a trend of increasing lacunarity L for the same sample as the image magnification increases (Table 1). A similar conclusion was presented in [24]. In contrast, as the image magnification increases, the calculated fractal dimension D tends to decrease. This indicates the mathematical imperfection of the obtained fractal figures, since for an ideal fractal, the fractal dimension should remain constant. This result is consistent across other samples as well. Therefore, it is appropriate to compare the fractal parameters of texture images for different samples only at the same magnification.

Table 1.

Fractal Characteristics of Composite Microstructures

Microscopy Type (SE, BSE)	Image Magnification	Fractal Dimension, *D*	Lacunarity, *L*
Sample №1			
SE	5k×	1.808±0.034	0.34±0.02
SE	10k×	1.790±0.035	0.36±0.02
SE	20k×	1.754+0.035	0.43±0.02
BSE	5k×	1.814±0.034	0.37±0.02
BSE	10k×	1.795±0.034	0.39±0.02
BSE	20k×	1.741±0.034	0.58±0.02
Sample №2			
SE	10k×	1.804±0.034	0.34 ±0.02
SE	20k×	1.777±0.034	0.41±0.02
SE	40k×	1.724±0.035	0.51±0.02
BSE	10k×	1.799±0.034	0.28±0.02
BSE	20k×	1.765±0.034	0.31±0.02
Sample №3			
SE	5k×	1.828±0.033	0.26±0.02
SE	10k×	1.812±0.035	0.29±0.02
SE	20k×	1.773±0.035	0.36±0.02
SE	40k×	1.736±0.033	0.46±0.02
BSE	20k×	1.748±0.034	0.35±0.02
Sample №4			
SE	10k×	1.821±0.037	0.26±0.02
SE	20k×	1.795±0.037	0.36±0.02
SE	40k×	1.744±0.035	0.50±0.02
BSE	10k×	1.817±0.034	0.22±0.02
BSE	20k×	1.777±0.034	0.28±0.02

Source: Calculations performed by the authors

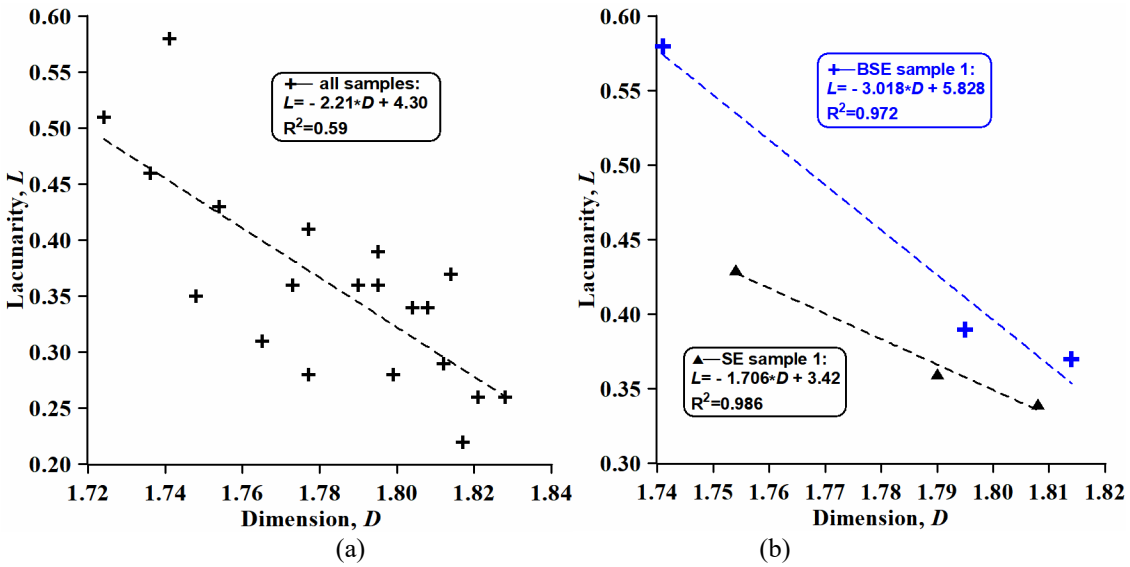

(a) (b)

Fig. 5. Correlation between fractal dimension and lacunarity based on the data from Table 1: (a) – linear relationship with a coefficient of determination $R^2 = 0.59$ for all images; (b) linear relationship with coefficients of determination for Sample №1 – $R^2 = 0.97$ for BSE microimages and R^2=0.99 for SE microimages.

3.1. Estimation of thermal conductivity of ZrB_2–C using fractal analysis

The obtained data allow us to explore possible correlations between the material's thermal conductivity coefficient *k* and the derived fractal parameters.

It is worth noting that SE images visually appear more three-dimensional and detailed. This is why such relief-type images are commonly presented in research studies. However, for our calculations, the ZrB_2 matrix in SE images may appear either light or dark gray, while graphite appears dark gray to black. When the image is converted to binary mode, these gray shades are

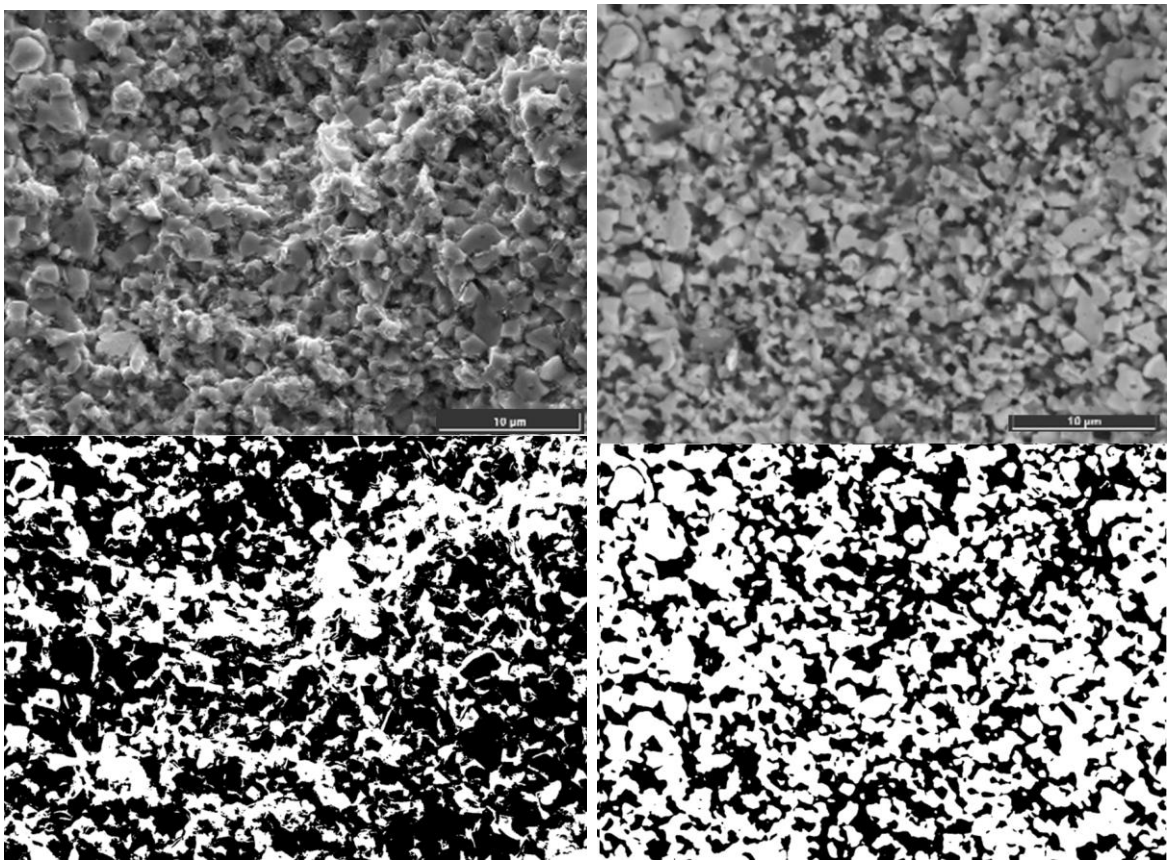

(a) (b)

Fig. 6. Microimages of the fracture surface of Sample № 2 at 10k× magnification: (a) in SE mode – before and after binarization; (b) in BSE mode – before and after binarization.

transformed into just two colors – and as a result, dark gray matrix grains may be interpreted as black zones, like the graphite itself. This can significantly alter the phase contours (Fig. 6a).

Therefore, BSE microimages were chosen for further thermal conductivity analysis. Although BSE images may appear visually less detailed and more averaged, the phase separation on them is more accurate: the light regions correspond to zirconium diboride, and the dark regions correspond to graphite (Fig. 6b).

To establish a correlation between lacunarity values and thermal conductivity, BSE-mode microimages with magnifications of 10k× and 20k× were selected. For Sample №3, no image was available at 10k× magnification (see Table 1).

Additionally, as revealed during visual analysis of the SE image of Sample №3, this sample contained residues of the starting powder or other impurities. Therefore, we believe that Sample №3 contains not two phases, but three (or more) phases. In the binarized image, the third phase appears white ─ the same as the matrix ─ which prevents unambiguous interpretation of the correlation between the composite's thermal conductivity and the lacunarity of the processed images.

For example, if the third phase consists of unreacted zirconium carbide powder, whose thermal conductivity is significantly lower than that of the synthesized composite components, the resulting error in correlation may be considerable.

The results (Fig. 7) indicate that the thermal conductivity of the synthesized composite increases as the lacunarity decreases. The lacunarity parameter reflects the heterogeneity of the composite's microstructure: lower lacunarity corresponds to a more homogeneous structure,

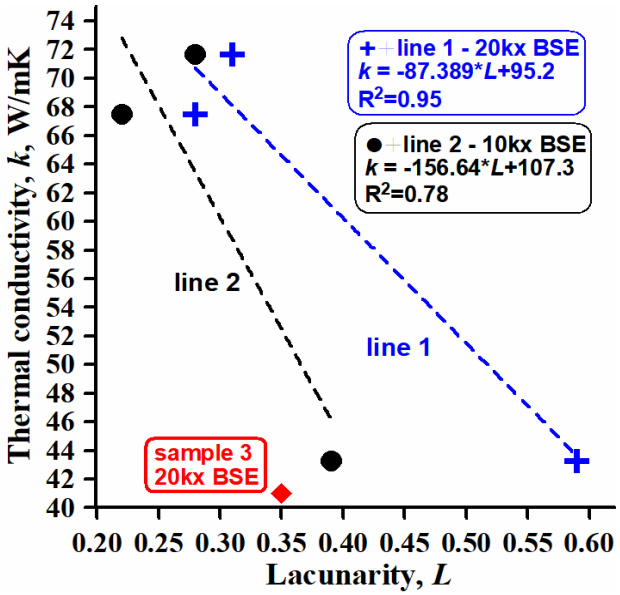

Fig. 7. Correlation between thermal conductivity and lacunarity for Samples №1, 2, and 4, showing high coefficients of determination: R^2=0.95 for approximation line 1 at 20k× magnification, R^2=0.78 for approximation line 2 at 10k× magnification. Sample №3 was excluded from the correlation analysis and is shown for completeness of description.

which facilitates more efficient heat transfer. This is the main finding of the present study. Among the presented images, the most uniformly distributed structures are observed in Samples № 2 and № 4.

Let us provide a microscopic interpretation of mentioned behaviour. A two-phase composite consists of a ZrB_2 phase and a graphite phase. In the case of a uniform distribution of phases, the grains of each phase are located at relatively short distances from one another, allowing thermal energy to transfer more efficiently. From this perspective, an interconnected network of a particular phase within the material will enable faster and more effective heat transfer. This is precisely what we observe in Samples № 2 and № 4, where a visible phase network is formed. The smaller the grains of the matrix phase and the more evenly distributed the phases, the more "connected" the networks of both the graphite and ZrB_2 phases become.

In contrast, Sample №1 exhibits large grains of the ZrB_2 phase and large, separately located graphite inclusions. Such a structure forms a composite in which an interconnected phase network is not formed, thus impeding heat transfer.

In other words, for a two-phase composite with isolated large grains, the propagation of thermal vibrations is more efficient within each material individually, but the overall heat flux is hindered at the grain and phase boundaries.

Conclusions

The fractal analysis method can be effectively applied to analyse the thermal conductivity of composite materials. A crucial condition for the efficacy of fractal analysis is the presence of visually distinguishable components within the composite material. The fractal approach is highly suitable for analysing the microstructure and thermal conductivity of two-phase synthesized composites, where the matrix and inclusions correspond to a binary image. However, in the case of three-phase composites, the applicability of this method is limited, especially when there are significant differences in the thermal conductivity of the individual phases.

For the two-phase ZrB_2–C composite, it is advisable to use the lacunarity parameter L for thermal conductivity estimation via fractal analysis, as it is more relevant and informative. The change in fractal dimension D was minor compared to the error margin of the *Box Counting* method. Nonetheless, a strong correlation between fractal dimension and lacunarity was demonstrated for the presented data.

In two-phase systems, BSE electron microscopy images should be preferred for fractal analysis. This choice simplifies binarization and enhances the reliability of fractal dimension and lacunarity calculations.

For zirconium diboride–graphite composites, thermal conductivity increases as lacunarity decreases, which corresponds to smaller grain sizes in the matrix and a more uniform phase distribution. Lower lacunarity characterizes a more homogeneous composite structure, which correlates with improved heat transfer.

The recommendation to use fractal analysis is especially valid in cases where direct sample acquisition is impractical — such as remotely obtained surface micrographs in radioactive environments, reactors, or situations requiring nondestructive testing.

Fractal analysis can serve as an effective tool to identify outlier samples that deviate from the main correlation trends. Significant deviations in fractal parameters within the studied group indicate atypical material behavior (or its fragment) and warrant additional examination.

Acknowledgements

The research is being conducted within the framework of the Research (Registration number 0125U000276) of the Laboratory of Composite Materials for Nuclear and Hydrogen Energy at the Institute of Applied Physics of NASU. The authors express their gratitude to Dr. Oleksii Popov (Institute of Applied Physics, Sumy, Ukraine; Institute of Materials Research, University of Huddersfield, UK) for providing the micrographs of the samples and the thermal conductivity data of the synthesized ZrB_2–C composite ceramic materials.

Shirinyan Aram – Doctor of Physical and Mathematical Sciences (PhD habil), Associate Professor, Head of Laboratory of Composite Materials for Nuclear-Hydrogen Energy;
Marynchenko Lolita – Candidate of Technical Sciences (PhD), Senior Research Fellow, Associated Professor of the Department of Bioenergy, Bioinformatics and Environmental Biotechnology;
Nizhelska Olena – Candidate of Biological Sciences (PhD), Research fellow, Laboratory of Composite Materials for Nuclear-Hydrogen Energy.

[1] A. Khomenko, E Khomenko, G Bagliuk, B Miedzinski, A Kozlowski, *Investigation of correlation between physical properties and microstructure geometrical parameters of Cr-Cu composite material used for vacuum arcing contacts, Mining–Informatics*, Automation and Electrical Engineering, Kyiv, 54(2), 29 (2016); https://journals.indexcopernicus.com/api/file/viewByFileId/235702.

[2] P. Budanov, E Khomiak, *Improving the system for monitoring the tightness of the cladding of the fuel element of a nuclear reactor*, Engineering [Mashynobuduvannja], 29, 32 (2022); https://jmash.uipa.edu.ua/index.php/jMASH/article/view/284/208.

[3] M.R.B. Dias, D. Dornelas, W.F. Balthazar, J.A.O. Huguenin, L. da Silva, *Lacunarity study of speckle patterns produced by rough surfaces*, Physica A: Statistical Mechanics and its Applications, 486, 328 (2017); https://doi.org/10.1016/j.physa.2017.05.022.

[4] A. Karperien, H. Ahammer, H. F. Jelinek, *Quantitating the subtleties of microglial morphology with fractal analysis*, Frontiers in cellular neuroscience, 7, 3 (2013); https://doi.org/10.3389/fncel.2013.00003.

[5] E.P. Pinto, M.A. Pires, R.S. Matos, R.R. M. Zamora, R.P. Menezes, R.S. Araújo, T.M. de Souza, *Lacunarity exponent and Moran index: A complementary methodology to analyze AFM images and its application to chitosan films*, Physica A: Statistical Mechanics and its Applications, 581, 126192 (2021); https://doi.org/10.1016/j.physa.2021.126192.
[6] A. Roy, E. Perfect, *Lacunarity analyses of multifractal and natural grayscale patterns*, Fractals, 22(03), 1440003 (2014); https://doi.org/10.1142/S0218348X14400039.
[7] F. Cervantes-Alvarez, J. J. Reyes-Salgado, V. Dossetti, J. L. Carrillo, *Thermal properties of composite materials with a complex fractal structure*, J. Phys. D: Appl. Phys., 47, 235303 (2014); https://doi.org/10.1088/0022-3727/47/23/235303.
[8] L. C. Feng, N. Xie, W. Z. Shao, L. X. Lu, L. Zhen, J. Zhao, *Thermal conductivity determination of conductor/insulator composites by fractal: Geometrical tortuosity and percolation*, Composites Part B: Engineering, 92, 377 (2016); https://doi.org/10.1016/j.compositesb.2016.02.046.
[9] V.V. Usov, M.D. Rabkina, N.M. Shkatuliak, T.S. Cherneva, *The fractal dimension of grain boundaries and mechanical properties of the oxygen cylinders metal*, Physicochemical Mechanics of Materials, 50(4), 117 (2014); http://nbuv.gov.ua/UJRN/PHKhMM_2014_50_4_19
[10] V. Ivanov, V. Pirozhkova, V. Lunev, *Research of structure and formation of nodular graphite inclusions in ductile cast iron*, Eastern-European Journal of Enterprise Technologies, 3(5(81)), 31 (2016); https://journals.uran.ua/eejet/article/view/69674/66776.
[11] D.M. Stefanescu, G. Alonso, P. Larranaga, E. De la Fuente, R. Suarez, *On the crystallization of graphite from liquid irone-carbone-silicon melts*, Acta Materialia, 107, 102 (2016); https://doi.org/10.1016/j.actamat.2016.01.047.
[12] M. Mróz, A. W. Orłowicz, M. Tupaj, M. Jacek-Burek, M. Radoń, M. Kawiński, *The Effect of Structure on Thermal Power of Cast-iron Heat Exchangers,* Archives of Foundry engineering, 20(1), 27 (2020); https://doi.org/10.24425/afe.2020.131278.
[13] C. Li, Y. Xu, Z. Jiang, B. Yu, P. Xu. *Fractal Analysis on the Mapping Relationship of Conductivity Properties in Porous Material*, Fractal and Fractional, 6(9), 527 (2022); https://www.mdpi.com/2504-3110/6/9/527.
[14] Z. Y. Du, M. L. Yang, Q. G. Liu, M. Yu, *Numerical investigation on Thermal Conduction in Fractal-like Porous Media*, Arch Environ Sci Environ Toxicol: AESET-109 (2019); https://www.gavinpublishers.com/assets/articles_pdf/1553244837article_pdf1275728101.pdf.
[15] W.G. Fahrenholtz, E.J. Wuchina, W.E. Lee, Y. Zhou (Editors), *Ultra-High Temperature Ceramics Materials for Extreme Environment Applications*, John Wiley & Son, 2014. ISBN:9781118700785 ; https://onlinelibrary.wiley.com/doi/book/10.1002/9781118700853.
[16] A.L. Chamberlain, W.G. Fahrenholtz, G.E. Hilmas, D.T. Ellerby, *High-strength zirconium diboride-based ceramics*, J. Am. Ceram. Soc., 87(6), 1170 (2004); https://doi.org/10.1111/j.1551-2916.2004.01170.x.
[17] G. J. K. Harrington, G. E. Hilmas, *Thermal Conductivity of ZrB2 and HfB2, Ultra-High Temp*. Ceram. Mater. Extrem. Environ. Appl., John Wiley & Sons, Ltd, 197 (2014); https://doi.org/10.1002/9781118700853.ch9.
[18] G.R. Peterson, R.E. Carr, E.E. Marinero, *Zirconium Carbide for Hypersonic Applications*, *Opportunities and Challenges*, Materials (Basel), 16(18), 6158 (2023); https://doi.org/10.3390/ma16186158.
[19] Yu. Zhao, Yi. Tao, K. Lin, J. Yang, J. Sha, Yu. Chen, *Experimental measurement of thermal conductivity along different crystallographic planes in graphite,* J. Appl. Phys., 128, 045118 (2020); https://doi.org/10.1063/5.0013474.
[20] C. Wood, D. Emin, P. E. Gray, *Thermal conductivity behaviour of boron carbides*, Physical Review B, 31(10), 6811 (1985); https://doi.org/10.1103/PhysRevB.31.6811.
[21] F.S. Moghanlou, M. Vajdi, J. Sha, A. Motallebzadeh, M. Shokouhimehr, M. S. Asl, *A numerical approach to the heat transfer in monolithic and SiC reinforced HfB2, ZrB2 and TiB2 ceramic cutting tools*, Ceram. Int., 45(13), 15892 (2019); https://doi.org/10.1016/j.ceramint.2019.05.095.
[22] O. Popov, J. Vleugels, E. Zeynalov, V. Vishnyakov, *Reactive hot pressing route for dense ZrB2-SiC and ZrB2-SiC-CNT ultra-high temperature ceramics*, Journal of the European Ceramic Society, 40(15), 5012 (2020); https://doi.org/10.1016/j.jeurceramsoc.2020.07.039.
[23] O. Popov, *Thermal conductivity and thermal shock resistance of TiB2-based UHTCs enhanced by graphite platelets*, Mater. Today Commun., 26, 101756 (2021); https://doi.org/10.1016/j.mtcomm.2020.101756.
[24] D. Ristanović, N. T. Milosević, *Fractal analysis: methodologies for biomedical researchers*, Theor Biol Forum, 105(2), 99 (2012); PMID: 23757956; https://pubmed.ncbi.nlm.nih.gov/23757956/
[25] O. Krit, A. Shirinyan, L Marynchenko, O. Nizhelska, *Assessment of Changes in the Texture of the Silicon Surface under the Influence of a Magnetic Field and High-Temperature Plastic Deformation Using Fractal Analysis*, Him. Fiz. Tehnol. Poverhni, 16 (3), 339 (2025); https://cpts.com.ua/index.php/cpts/article/view/805/804.

А.С. Шірінян[1], Л.В. Маринченко[2], О.І. Ніжельська[1]

Фрактальний підхід до оцінки теплопровідності композитних керамічних матеріалів ZrB_2–C

[1]*Лабораторія композитних матеріалів атомно-водневої енергетики, Інститут прикладної фізики НАН України, м. Суми, Україна, aramshirinyan@ukr.net*
[2]*Кафедра біоенергетики, біоінформатики та екобіотехнології, Національний технічний університет України "Київський політехнічний інститут імені Ігоря Сікорського", м. Київ, Україна, lolitamar@ukr.net*

Актуальною проблемою матеріалознавства є контрольоване використання керамічних композитних матеріалів за високих температур у сучасних технологіях, зокрема в ядерній фізиці, атомній енергетиці та авіакосмічному і ракетному машинобудуванні. У статті досліджено зв'язок між мікроструктурою гетеромодульного керамічного композиту на основі дибориду цирконію і графіту, отриманого методом високотемпературного реакційного синтезу, та його теплопровідними властивостями. Методологія дослідження ґрунтується на використанні фрактального аналізу мікрозображень, що дає змогу кількісно оцінити просторову неоднорідність структури. Показано, що параметр лакунарності є більш інформативним для оцінки теплопровідності, ніж фрактальна розмірність, з огляду на його чутливість до розподілу фаз. Встановлено, що для двофазних композитів із суттєвим контрастом теплопровідності компонентів (наприклад, цирконієвий диборид – графіт) зниження лакунарності графітової фази корелює зі зростанням ефективної теплопровідності матеріалу. Окремо підкреслено доцільність використання BSE-зображень для підвищення точності обчислень. Зроблено висновок про ефективність фрактального підходу для аналізу мікроструктури та прогнозування коефіцієнту теплопровідності синтезованих двофазних керамічних композитів за даними електронної мікроскопії.

Ключові слова: керамічні композити, карбід бору, карбід цирконію, диборід цирконію, графіт, мікроструктура, фрактальний аналіз, теплопровідність, лакунарність, енергетика.